Published in final edited form as:
J Phys Chem B. 2010 June 10; 114(22): 7656–7661. doi:10.1021/jp101004k.

Thermodynamic Characterization of DNA with 3-Deazaadenine and 3-Methyl-3-Deazaadenine Substitutions: The Effect of Placing a Hydrophobic Group in the Minor Groove of DNA

Manjori Ganguly[†], **Ruo-Wen Wang**[†], **Luis A. Marky**[‡], and **Barry Gold**[†,*]

[†]Department of Pharmaceutical Sciences, University of Pittsburgh, Pittsburgh, PA 15261, USA

[‡]Department of Pharmaceutical Sciences, University of Nebraska Medical Center, Omaha, NE 68109-6025, USA

Abstract

In many high-resolution structures of DNA there are ordered waters associated with the floor of the minor groove and extending outward in several layers. It is thought that this hydration structure, along with cations, reduces the Coulombic repulsion of the interstrand phosphates. In previous studies, the replacement of the 3-N atom of adenine with a C-H to afford 3-deazaadenine was shown to decrease the thermodynamic stability of DNA via a reduction in the enthalpic term. Using spectroscopic and calorimetric methods, we report herein a rigorous examination of the thermodynamics of DNA with 3-deazaadenine modifications, and report for the first time how the presence of a minor groove methyl group, i.e., 3-methyl-3-deazaadeine, affects DNA stability, hydration and cation binding. The methylation of adenine at the N3-position to yield N3-methyladenine represents an important reaction in the toxicity of many anticancer compounds. This minor groove lesion is unstable and cannot be readily studied in terms of its effect on DNA stability or structure. Our studies show that 3-methyl-3-deazaadenine, an isostere of N3-methyladenine, significantly destabilizes DNA ($\Delta\Delta G > 4$ kcal•mol^{-1}) due to a significant drop in the enthalpy (ΔH) term, which is associated with a lower hydration of the duplex relative to the unfolded state.

Introduction

In its simplest state, DNA is an ensemble of nucleic acids, water and salts, and the structure of the ensemble is dynamically dependent on all three components, e.g., sequence of nucleic acid bases, type and concentration of salts and the level of hydration.[1] As a result, DNA can adopt multiple conformations upon environmental changes that differ subtly from each other, such as B-DNA *vs*. B′-DNA, or dramatically, as B-DNA *vs*. A- or Z-DNA.[2] These alterations involve changes in the conformation of the bases and sugars, and in the concomitant reorganization of water molecules and cations.

To explore how alterations in hydration and cation binding affect structure and stability, studies have been performed on DNA that is site specifically modified with base analogs that are designed to affect the interactions of water and cations at the edges of the bases in the major and minor grooves. It turns out that even modest changes in DNA structure alter the thermodynamic stability, although associated structural changes are not always obvious from crystal structures or low temperature NMR studies. For example, the crystal[3] and high-resolution NMR[4] structure of 5'-CGCGAATTC**Z**CG (Z = 7-deazaguanine; c^{7}G) is

*To whom correspondence should be addressed (goldbi@pitt.edu).

indistinguishable from the unmodified sequence with one notable exception; a highly conserved cation-binding site is missing in the crystal structure.[3] Despite the similarity in the crystal structure, the temperature-dependent imino proton NMR spectrum showed a specific increase in exchange of imino proton of the C•G pair that flanks the c^7G modification toward the 3′-terminus.[4] The exchange rate for the c^7G•C base pair was the same as in the natural sequence. Thermodynamic studies revealed a slight drop in $\Delta\Delta G$ vs. the natural sequence, but with a significant change in the enthalpic term that was only partially compensated by entropic stabilization. Analysis of the relative change in hydration and cation binding between the duplex and random coil states for the natural and c^7G modified sequence provided an important insight into the origin of the thermodynamic effects of the modification. The DNA with the c^7G showed, after normalizing for the number of base pairs, a decrease of 10 water molecules per mole of duplex in the hydration level relative to the natural sequence. This calculates to a reduction of 5 water molecules per modification. The release of counterions from the c^7G substituted duplex is also lower. A similar scenario has also been observed with the corresponding 7-deazaadenine (c^7A) modification (manuscript in preparation). Of note, is that tethering a basic amine onto the 7-position of c^7G (i.e., 7-NH_2CH_2-c^7G) resulted in a duplex with thermodynamic properties similar to the unmodified DNA, while an isosteric hydroxyl group was destabilizing similar to the c^7G DNA.[5] In this case the cationic 7-NH_2CH_2-c^7G substitution had a small effect on hydration and cation binding *vs*. the unmodified DNA.

Because of our observation that changes in the major groove cause an enthalpic destabilization that is associated with a reduction in duplex hydration and cation binding, we have performed thermodynamic measurements on DNA with minor groove alterations, i.e., a c^3A residue. In addition, we included studies on 3-methyl-3-deazaA (3-Me-c^3A) to determine the effect of a hydrophobic group in the minor groove. The 3-Me-c^3A serves as a stable isostere of N3-methyladenine (3-MeA) that is a common methylation adduct formed by many carcinogens and anticancer drugs, e.g., temozolomide.[6-10]

The substitution of a single c^3A into 5′-d(CG-c^3A-TTGCG)•3′-d(GCTAACGC) at 120 mM Na^+ has been shown to be destabilizing (~1.4 kcal/mol) by UV melting experiments.[11] Multiple substitutions caused further destabilization and a significant drop in the van't Hoff ΔH term. It was suggested that the instability was due to the pK_a of N-1 in c^3A that would make it more prone to protonation, which would disrupt Watson-Crick H-bonding to its dT partner. In addition, disruption of the structure of minor groove hydration was also proposed as a potential destabilizing factor. A sequence-dependent effect of c^3A on the flexibility of an intrinsically bent A-tract has also been noted.[12] The reduction in bending was observed when the c^3A was placed on the 3′-side of an A_6 tract. It was suggested that the relative hydrophobicity of c^3A might interfere with minor groove hydration and this could reduce bending at the A-tract.[12] However, no studies have been performed that actually measure changes in hydration induced by the c^3A or 3-Me-c^3A residues. In studies presented herein, an adenine at positions -4 and -6, respectively, in the self-complementary duplexes 5′-d(GAGAGCGCTCTC)-3′ and 5′-d(CGCGAATTCGCG)-3′ was replaced by c^3A or 3-Me-c^3A. The results show that there are significant thermodynamic differences between the methylated and unmethylated deazaadenines. The origin of the difference is discussed in terms of the fundamental role of minor groove ions and water molecules in the stabilization of the DNA architecture.

Experimental Methods

Materials

All oligodeoxynucleotides (ODNs) were synthesized by Invitrogen (Frederick, MD). The phosphoramidite derivative of 3-Me-c^3A was prepared as previously described.[13] The phosphoramidite of c^3A was obtained commercially from Glen Research (Sterling, VA). The modified oligomers were purified using a 10 × 250 mm Phenomenex 5 μm phenyl-hexyl reverse

phase HPLC column (Torrance, CA) equilibrated with 0.1 M diethylammonium acetate (pH 7.0). After desalting by gel-permeation chromatography using a Sephadex G-25 column, the sample was lyophilized to dryness. The samples were characterized by MALDI-TOF-MS. The dry oligomers were then dissolved in the appropriate buffer.

The concentrations of the oligomer solutions were determined at 80 °C using 260 nm and extinction coefficient ~ 1.11×10^5 M^{-1} cm^{-1} (ODN; 1-3, 4, 6 and 7), and 1.05×10^5 M^{-1} cm^{-1} (ODN-5; hairpin) at 260 nm and 25 °C assuming similar extinction coefficients for 3-Me-c^3A and c^3A. These values are obtained from the molar absorptivity at 25 °C, and derived from the tabulated values of the dimers and monomer bases,[14,15] and extrapolated from high temperatures using the upper portions of the UV melting curves, following procedures described earlier.[16] All measurements were performed in buffer solutions consisting of 10 mM sodium phosphate, adjusted to the appropriate salt and osmolyte concentrations with NaCl and ethylene glycol, respectively.

UV-Spectroscopy

Absorption vs. temperature profiles (UV melts) for each duplex were measured at either 260 nm and/or 275 nm using a thermoelectrically controlled Varian Cary 300 spectrophotometer (Palo Alto, CA), interfaced to a PC computer for data acquisition and analysis. The temperature was scanned at heating rates of 1.00 °C/min. Melting curves as a function of strand concentration (4–70 μM) were obtained to check for the molecularity of each molecule. Additional melting curves were obtained as a function of salt and osmolyte concentration to determine the differential binding of counterions and water molecules that accompanies their helix coil transitions.

UV melts were measured in the salt range of 10−200 mM NaCl at pH 7.0, and at a constant total strand concentration of 7 μM, to determine the differential binding of counterions, Δn_{Na^+}, which accompanied their helix−coil melting. This linking number was measured experimentally with the assumption that counterion binding to the helical and coil states of each oligonucleotide took place with a similar type of binding using the relationship:[17,18]

$$\Delta n_{Na^+} = 0.483 \left[\Delta H_{cal} / R (T_M)^2 \right] (\partial T_M / \partial \log [Na^+]) \quad \text{Eq. 1}$$

The numerical factor corresponded to the conversion of ionic activities into concentrations. The first term in parentheses, ($\Delta H_{cal}/RT_M^2$), was a constant determined directly from DSC experiments, where R was the gas constant. The second term in parenthesis was determined from UV experiments from the dependencies of T_M on salt concentration.

For the determination of Δn_w, UV melts were measured in the ethylene glycol concentration range of 0.5- 3.0 m at pH 7.0 and 10 mM NaCl, and at a constant total strand concentration of 7 μM. The osmolalities of the solutions were obtained with a Wescor Vapro vapor pressure osmometer, Model 5520 (Logan, UT). These osmolalities were then converted into water activities, a_w, using the following equation:[19]

$$\ln a_w = -(Osm/M_w) \quad \text{Eq. 2}$$

where Osm is the solution osmolality and M_w is the molality of pure H_2O, equal to 55.5 mol/kg H_2O. Differential binding of water, Δn_w, was calculated using the relationship:[17,18]

$$\Delta n_w = 0.434 \left[\Delta H_{cal} / R (T_M)^2 \right] [\partial T_M / \partial \log a_w] \quad \text{Eq. 3}$$

The $[\Delta H_{cal}/R(T_M)^2]$ term used in the determination of Δn_w was derived from the 100 mM salt concentration and the slope $(\partial T_M/\partial \log a_W)$ was calculated from the 10 mM salt data.

Differential Scanning Calorimetry

Heat capacities vs. temperature profiles were measured with a VP-DSC differential scanning calorimeter (Microcal Inc., Northampton, MA). The dry oligodeoxynucleotides were dissolved in 10 mM sodium phosphate buffer (pH 7.0) and adjusted to the desired ionic strength with NaCl for all unfolding experiments. The heat capacity profile for each DNA solution was measured against a buffer solution. In a typical experiment the reaction and the reference cells were each filled with 0.75 mL of solution. Temperature was scanned from 0 to 100 °C at a rate of 0.75 °C/min. The experimental curve was normalized by the heating rate, and a buffer vs. buffer scan was subtracted and normalized for the number of moles. The resulting curves were then analyzed with Origin version 7.0 (Microcal); their integration ($\int \Delta C_p \, dT$) yielded the molar unfolding enthalpy (ΔH_{cal}), which was independent of the nature of the transition.[16,20] The molar entropy (ΔS_{cal}) was obtained similarly, using $\int(\Delta C_p/T)\, dT$. The free energy change at any temperature T was then obtained with the Gibbs equation:

$$\Delta G^{o}(T) = \Delta H_{cal} - T\Delta S_{cal}.$$

Circular Dichroism

Circular dichroism (CD) measurements were conducted on a Jasco(model J-815) CD spectrometer (Easton, MD). The spectrum of each duplex was obtained using a strain-free 1 cm quartz cell at low temperatures to ensure 100% duplex formation. Typically, 1 OD of a duplex sample was dissolved in 1 mL of a buffer containing 10 mM sodium phosphate (pH 7.0). The reported spectra correspond to an average of three scans from 220 to 350 nm at a wavelength step of 1 nm.

Results

UV melting studies

The unfolding of duplexes was studied by temperature-dependent UV spectroscopy. Absorption spectra at low and high temperatures revealed a higher hyperchromic effect at 260 nm than other wavelengths for all the oligomers (data not shown). This was chosen as the optimum wavelength for all UV melting studies. Typical UV melting curves are shown in Figure 1. All the curves follow the characteristic sigmoidal behavior for the unfolding of a nucleic acid helix structure. The helix-coil transition of ODNs 1-3 exhibit monophasic transition under all conditions studied. T_M values were determined from the first derivative of the melting curves and shape analysis. The T_M values follow the order: ODN-1 (41.0 °C) > ODN-2 (34.9 °C) > ODN-3 (30.3 °C) in 10 mM salt and ODN-1 (59.5 °C) > ODN-2 (51.2 °C) > ODN-3 (47.9 °C) in 100 mM salt at a DNA concentration of 10 μM. The presence of c^3A residues in DNA reduces the T_M confirming earlier reports.[11] The data also indicates the lower stability of duplexes with 3-Me-c^3A·T base pairs. ODN-3 also shows lower hyperchromicity which is indicative of lower stacking contributions. To confirm the molecularity of each complex, melting curves were obtained as a function of strand concentration. Strand concentration-dependent experiments done at both 10 mM and 100 mM salt concentrations showed an increasing T_M with an increase in the total strand concentration in the range of ~ 4-120 μM (Figure 2). This is evidence of duplex to random coil denaturation.

Circular dichroism

The average solution conformation of the oligomers was obtained using CD spectroscopy, which was performed in low salt conditions (10 mM salt). All spectra show a positive Cotton effect around 290 nm and a negative Cotton effect around 250 nm, which are characteristics of a right-handed helix in the B-conformation. The CD spectra of ODNs 1-3 are shown in Figure 3. The intensities of the negative band near 250 nm reflect base stacking contributions. The intensity of the differential CD band at 250 nm for ODN-3 is 75% lower relative to corresponding band for ODN-1 and 45% lower relative to ODN-2. These changes suggest a partial disruption of base stacking due to the presence of methyl group in 3-Me-c^{3}A, and consistent with its lower hyperchromicity.

DSC unfolding studies of duplexes

The DSC melting curves for ODNs 1-3 are shown in Figure 4a. Additional DSC curves for ODNs 4-6 are shown in Figure 4b and the corresponding thermodynamic parameters are provided in Table 2. The reported thermodynamic values are an average of the analysis of three consecutive scans. ODNs 1-3 exhibit monophasic melting profiles at both 10 mM and 100 mM salt concentrations confirming their unfolding through a duplex to random coil transition as seen in the UV studies. The T_M values at the concentrations used in the DSC experiments follow the order: ODN-1 (48.7 °C) > ODN-2 (45.2 °C) > ODN-3 (38.8 °C) in 10 mM salt and ODN-1 (66.1 °C) > ODN-2 (61.3 °C) > ODN-3 (58.8 °C) in 100 mM salt. ODNs 4-7 unfold via biphasic transitions at 10 mM salt. The DSC thermogram of ODN-4, as reported earlier, has a broad first transition and a sharp second transition that is typical of the helix → hairpin → random coil transitions of this Dickerson-Drew dodecamer duplex.[21] DSC thermograms for ODN-6 and -7 reveals biphasic curves with a small shoulder at low temperature for the first transition and a broad second transition at higher temperature with second transition T_M similar to that of the T_M of hairpin ODN-5 (Table 2) reported in the literature.[4] Enthalpies reported in Table 2 were determined by deconvolution of the DSC graphs.

Analysis of thermograms reveal that ODN-2, which has two c^{3}A substitutions in the molecule, has an endothermic enthalpy of 75.8 kcal/mol that is similar to the unmodified oligomer, ODN-1, in 10 mM NaCl (Table 2). This pattern remains unchanged at the higher salt concentration of 100 mM NaCl. Introduction of two 3-Me-c^{3}A residues in ODN-3 results in a reduction of enthalpy by 39.2 kcal/mol and 52.4 kcal/mol relative to unmodified ODN-1 (Table 2) in 10 and 100 mM buffer, respectively. The data suggest that incorporation of this methyl group destabilizes duplex structure at both low and high salt concentrations. This contrasts with the placement of methyl groups in the major groove where dT•dA base pairs are more stable than dU•dA.[22]

On the other hand, incorporation of c^{3}A and 3-Me-c^{3}A residues in the AATT core of ODN-4 stabilizes the hairpin conformation. Analysis of the data does not show any significant change in enthalpy when compared with the unmodified hairpin molecule ODN-5, indicating a similar extent of duplex structure.

The DSC melting curves at the two salt concentrations provides an indirect measurement of the heat capacity (ΔC_p) in the unfolding of each duplex. The ΔC_p (cal/°K•mol) values measured at 10 and 100 mM NaCl for ODN-1, ODN-2 and ODN-3 are 793, 969 and 30, respectively. This heat capacity effect indicates that ODN-3 behaves more like a random coil. Assuming that hydration of the random coils at high temperature will be similar for all of the sequences, by definition the more hydrophilic DNA will release more waters upon denaturation. This is consistent with the measured heat capacity effect. Therefore, the greater release of water from ODN-1 and ODN-2 duplexes means that they are more hydrophilic than ODN-3.

Thermodynamic profiles for the formation of duplex

The complete thermodynamic profiles for the folding of each duplex at 20 °C are shown in Table 2. Analysis of the thermodynamic data indicates that the stable formation of each duplex is accompanied by favorable Gibbs free energy, which results from the characteristic compensation of a favorable enthalpy term with an unfavorable entropy term. The favorable enthalpies arise from the formation of base-pairs and base pair stacks, uptake of electrostricted water and release of structural water. The unfavorable entropy contribution is mainly due to the ordering of a random coil into a duplex structure, condensation of counterions and immobilization of water molecules.

Relative to the unmodified oligomer ODN-1, both c^3A and 3-Me-c^3A modified oligomers were destabilized at low and high salt concentrations. The inclusion of two c^3A modifications inODN-2 yielded a mild decrease in ΔG of 0.9 and 1.2 kcal/mol in 10 mM and 100 mM NaCl, respectively, a value that is similar to the destabilization observed in a different sequence.[11] In contrast, substitution of two 3-Me-c^3A residues results in a marked reduction of ΔG by 4.5 and 7.9 kcal/mol in low and high salt, respectively.

Differential association of counterions

UV melting curves as a function of Na^+ concentration were performed in the 10 to 200 mM NaCl range to examine the thermodynamic association of counterions with the DNA duplexes. The T_M of ODNs 1-3 linearly increased with salt concentration (data not shown), consistent with the fact that the duplex states have higher charge density parameters. The T_M dependence on salt concentration is shown in Figure 5. Equation 1 was used to calculate Δn_{Na+} values shown in Table 2, using the slopes $\partial T_M/\partial \log [Na^+]$ from Figure 5 in conjunction with the $\Delta H/R(T_M)^2$ terms. Data indicates that in low salt, the Na^+ uptake (mol Na^+ per mol duplex) were in the order ODN-1 (3.4) > ODN-2 (3.0) > ODN-3 (1.4) and a similar pattern ODN-1 (3.6) > ODN-2 (3.2) > ODN-3 (1.2) was observed in the higher salt concentration of 100 mM (Table 2).

Assuming that the random coil states of the single strand oligomers are thermodynamically equivalent at higher temperature, it can be concluded that the introduction of c^3A or 3-Me-c^3A into the duplex DNA causes a decreased association of counterions. For instance, there is a $\Delta\Delta n_{Na+}$ of ~0.4 between ODN-1 and ODN-2 at 10 and 100 mM NaCl, respectively. Introduction of the methyl group causes a larger $\Delta\Delta n_{Na^+}$ of 1.6 and 2.0 between the pair ODN-2 and ODN-3 at low and high salt, respectively.

Differential association of water molecules

UV melting curves as a function of osmolyte (ethylene glycol) concentration were performed in the 0.5-3.0 m range at 10 mM salt concentration in order to determine the thermodynamic association of water molecules to DNA duplexes. Increasing the concentration of ethylene glycol (decreasing water activity) had a marginal effect on the T_M. UV melting curves show that the T_Ms of the dodecamers ODNs 1-3 linearly decreased with increasing osmolyte concentrations i.e., decreasing activity of water (data not shown). The T_M dependence on water activity of dodecamers is shown in Figure 6. The values for the formation of each duplex in 10 mM NaCl are shown in Table 2. Equation 3 was used to calculate Δn_w values shown in Table 2, using the slopes $\partial T_M/\partial \log a_w$ from Figure 6 in conjunction with the $\Delta H/R(T_M)^2$ terms. Water uptake, expressed as mol H_2O per mol duplex, measured in low salt, were in the order: 41 for ODN-1 > 35 for ODN-2 > 24 for ODN-3. A similar pattern was observed in the higher salt concentration of 100 mM: 43 for ODN-1 > 28 for ODN-2 > 21 for ODN-3.

The overall effect, again assuming that the random coil state of all the duplexes behave similarly at higher temperature, is that the substitution of c^3A and 3-Me-c^3A into the duplex DNA causes

a decreased association of water molecules. Specifically, there is a $\Delta\Delta n_w$ of 6 and 11 between ODN-1 and ODN-2 at 10 mM and 100 mM NaCl, respectively, and $\Delta\Delta n_w$ of 11 and 17 between the pair ODN-2 and ODN-3 at low and high salt, respectively.

Discussion

The minor groove of DNA in the relatively few crystal structures that have been solved with high resolution show a well defined hydration scheme where waters are layered from the floor of the groove on outward toward the bulk solvent. This is especially true in sequences that have narrow minor grooves, such as those with an A_2T_2 or A_3T_3 central core.[23-25] There is some debate whether the A/T rich sequences, without amino groups that project into the minor groove, drives the structure which in turn allows a well-defined hydration spine or whether the structural water in the narrow groove allows the groove to further narrow.

Our thermodynamic studies cannot directly answer this question. However, the lack of the 3-nitrogen atom in c^3A has a potent impact on stability of the 5′-CGCGA-(c^3A)-TTCGCG sequence (ODN-6) as it preferentially hairpins (Figure 4b). The same preference for the hairpin structure for the 5′-CGCGA-(3-Me-c^3A)-TTCGCG sequence (ODN-7) is observed in the DSC experirments (Figure 4b). The unmodified dodecamer (ODN-4), with it's A/T rich central core, exists as a mixture of hairpin and duplex (Figure 4b). The ΔG, ΔH and $T\Delta S$ values for the true hairpin (ODN-5) are very similar to those for ODN-6 and -7. In all cases, the decrease in the number of base pairs from 12 to 4, and resulting decrease in base stacking, causes a significant reduction in the ΔH term. The small differences that exist between ODNs 5-7 can be attributed to differences from the modifications in the loop regions. To avoid the formation of hairpin structures, which complicate the analysis, we chose a self-complementary sequence (5'-GAGAGCGCTCTC) with a G/C rich center that tends not to hairpin. In addition, we introduced the c^3A or 3-Me-c^3A lesions at position-4 that will not promote the hairpin structure. Therefore, the thermodynamic parameters presented for ODNs 1-3 are for the unfolding of the duplex structure. The observed increase in T_M with increasing strand concentration is an example of proof of duplex formation. In the 5′-GAG-(c^3A)-GCGCTCTC and 5′-GAG-(3-Me-c^3A)-GCGCTCTC sequences the impact of c^3A and 3-Me-c^3A are still apparent, with the latter being highly destabilizing relative to the natural sequence by 4.5 and 7.9 kcal/mol at low and high salt, respectively. If disruption of the hydration structure near the floor of the groove by the hydrophobic methyl group is responsible for the change in ΔG then the hydration of ODN-3 would be expected to be lower than for ODN-2 and ODN-1. This is certainly the case with a $\Delta\Delta n_W$ of 17 water/mol DNA for ODN-3 vs. ODN-1. This calculates to ~9 H_2O per mol DNA per lesion. Interestingly, neither the enthalpy term nor the hydration parameter for ODN-3 is particularly sensitive to the salt concentration. The inclusion of the minor groove methyl group also causes a major reduction in cation binding (~2.2 Na^+/mol) or 1.1 Na^+/mol per 3-Me-c^3A residue, assuming a localized effect. Clearly, the hydration effect is significant and might be the major driving force for the observed reduced enthalpy ($\Delta\Delta H°$ ~ 40 kcal/mol). The change in hydration may also (directly or indirectly) afford reduced base-pair stacking contributions. The band intensities at 250 nm in CD data are consistent with some reduction in base stacking in ODN-3 even at low temperature.

The differential thermodynamic profiles obtained indicate that the A → c^3A substitution yielded marginal changes in ΔG, ΔH and ΔS, lower uptake of ions (0.2 per lesion corresponding to the loss of one ion site) and a marginal release of water (3/lesion). In contrast, the dA → 3-Me-c^3A substitution yielded substantial changes in all thermodynamic parameters. Comparison of the signs of $\Delta\Delta G$ (i.e., $\Delta\Delta H$-$\Delta T\Delta S$) and $\Delta\Delta V$ yields insight about the type of water released.[26] Similar signs for $\Delta\Delta G$ and $\Delta\Delta V$ indicate the participation of electrostricted water, while opposite signs indicate structural (i.e., hydrophobic) water. This is based upon the release of heat in the immobilization of electrostricted water where the water dipoles are

compressed, while the energetic contribution for the release of structural water is close to zero, or even slightly positive due to improved packing around hydrophobic groups that eliminates void spaces. The data (Tabale 2) indicate that the c^3A modification results in the participation of electrostricted water. In contrast, the placement of a hydrophobic methyl group in 3-Me-c^3A results in a decrease in electrostricted water.

N3-methyladenine (3-MeA) is a cytotoxic but weakly mutagenic lesion that is formed by the reaction of DNA with a number of environmental and endogenous methylating agents, as well as by methylating anticancer drugs.[6-10] Because the adduct is hydrolytically unstable, it has been difficult to study its effects in biochemical and biological systems. Since 3-Me-c^3A is a stable isostere of 3-MeA it has been used as a surrogate in recent studies that show it to be a potent block of DNA polymerization.[27] Although 3-Me-c^3A, and presumably 3-MeA, can form a normal Watson-Crick base pair with T, the studies presented herein indicate that this may not be the case. We propose that the thermodynamic instability induced by the minor groove methyl group will allow DNA repair glycosylase enzymes to rapidly find and remove the 3-MeA adduct. The instability induced by the methyl group may also be, in part, responsible for their inhibition of DNA polymerases when 3-MeA (Settles and Gold, unpublished) or 3-Me-c^3A [27] are in the template strand. We have preliminary evidence that 3-Me-c^3A can be by-passed within A-tracts due to it becoming extrahelical during polymerization (Settles and Gold, unpublished).

Conclusion

It has been demonstrated that relatively subtle changes in the structure of a DNA base, in this case a C-H or C-CH_3 group in the minor groove in place of the aromatic nitrogen at the N3-position of adenine, can have a dramatic effect on the enthalpic and entropic contributions to thermodynamic stability. The dynamic change in DNA appears to be associated with DNA hydration and cation association. This appears to be a common scenario; changes to the natural Watson-Crick base pairs reduces stability due to a loss of enthalpic stabilization that is associated with reduced hydration and cation binding.[4,5]

Acknowledgments

This work was supported by NIH grant CA29088 (BG).

References

1. Saenger, W. Principles of Nucleic Acid Structure. Springer-Verlag Inc.; New York: 1984.
2. Leslie AG, Arnott S, Chandrasekaran R, Ratliff RL. Journal of Molecular Biology 1980;143:49–72. [PubMed: 7441761]
3. Wang F, Li F, Ganguly M, Marky LA, Gold B, Egli M, Stone MP. Biochemistry 2008;47:7147–7157. [PubMed: 18549246]
4. Ganguly M, Wang F, Kaushik M, Stone MP, Marky LA, Gold B. Nucleic Acids Res 2007;35:6181–6195. [PubMed: 17855404]
5. Ganguly M, Wang R-W, Marky LA, Gold B. J. Am. Chem. Soc 2009;131:12068–12069. [PubMed: 19663509]
6. Bartsch H, Ohshima H, Shuker DE, Pignatelli B, Calmels S. Mutat. Res 1990;238:255–267. [PubMed: 2188123]
7. Hecht SS. Mutat. Res 1999;424:127–142. [PubMed: 10064856]
8. Bennett RA, Pegg AE. Cancer Res 1981;41:2786–2790. [PubMed: 6454479]
9. Tentori L, Graziani G. Curr. Med. Chem 2002;13:1285–1301. [PubMed: 12052167]
10. Newlands ES, Stevens MF, Wedge SR, Wheelhouse RT, Brock C. Cancer Treat Rev 1997;23:35–61. [PubMed: 9189180]

11. Lever C, Li X, Cosstick R, Ebel S, Brown T. Nucleic Acids Res 1993;21:1743–1746. [PubMed: 8493091]
12. Seela F, Grein T. Nucleic Acids Res 1992;20:2297–2306. [PubMed: 1630898]
13. Irani RJ, SantaLucia J. Nucleosides, Nucleotides and Nucleic Acids 2002;21:737–751.
14. Cantor CR, Warshow MM, Shapiro H. Biopolymers 1970;9:1059–1077. [PubMed: 5449435]
15. Marky LA, Blumenfeld KS, Kozlowski S, Breslauer KJ. Biopolymers 1983;22:1247–1257. [PubMed: 6850063]
16. Marky LA, Breslauer KJ. Biopolymers 1987;26:1601–1620. [PubMed: 3663875]
17. Cantor, CR.; Schimmel, PR. Biophysical Chemistry. W.H. Freeman and Company; New York: 1980.
18. Kaushik M, Suehl N, Marky LA. Biophysical Chemistry 2007;126:154–164. [PubMed: 16822606]
19. Courtenay ES, Capp MW, Anderson CF, Record MTJ. Biochemistry 2000;39:4455–4471. [PubMed: 10757995]
20. Rentzeperis D, Marky LA, Dwyer TJ, Geierstanger BH, Pelton JG, Wemmer DE. Biochemistry 1995;34:2937–2945. [PubMed: 7893707]
21. Shikiya R, Li JS, Gold B, Marky LA. Biochemistry 2005;44:12582–12588. [PubMed: 16156670]
22. Soto AM, Gmeiner WH, Marky LA. Biochemistry 2002;41:6842–6849. [PubMed: 12022889]
23. Wing R, Drew H, Takano T, Broka C, Tanaka S, Itakura K, Dickerson RE. Nature 1980;287:755–758. [PubMed: 7432492]
24. Drew HR, Dickerson RE. J. Mol. Biol 1981;151:535–556. [PubMed: 7338904]
25. Woods KK, Maehigashi T, Howerton SB, Sines CC, Tannenbaum S, Williams LD. J. Am. Chem. Soc 2004;126:15330–15331. [PubMed: 15563130]
26. Marky LA, Kupke DW. Methods Enzymol 2000;323:419–441. [PubMed: 10944762]
27. Plosky BS, Frank EG, Berry DA, Vennall GP, McDonald JP, Woodgate R. Nucleic Acids Res 2008;36:2152–2162. [PubMed: 18281311]

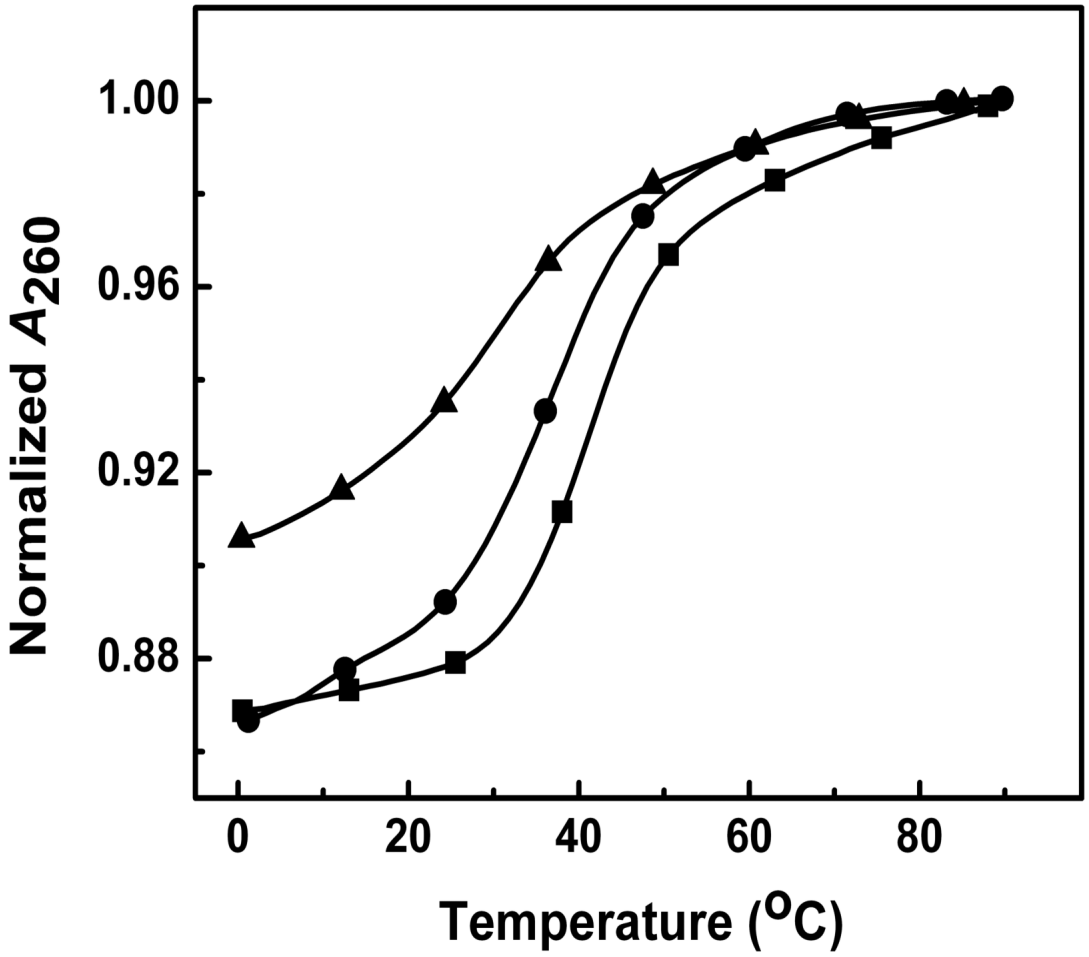

Figure 1.
UV melting curves in 10 mM sodium phosphate buffer (pH 7.0) at ~ 10 μM total strand concentration at 260 nm for ODN-1 (■), ODN-2 (●) and ODN-3 (▲).

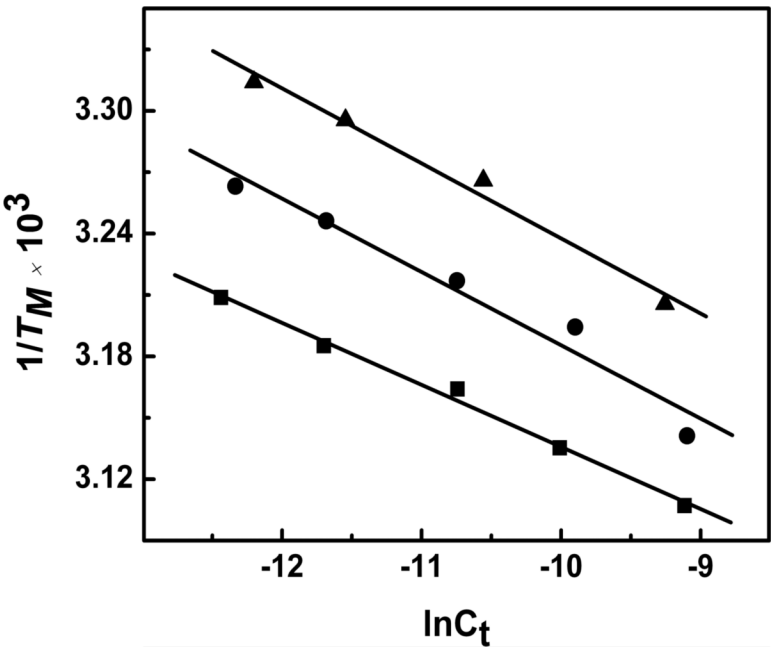

Figure 2.

T_M dependence on strand concentration for duplexes in 10 mM sodium phosphate buffer (pH 7.0), 4-120 μM strand concentration for ODN-1 (■), ODN-2 (●) and ODN-3 (▲).

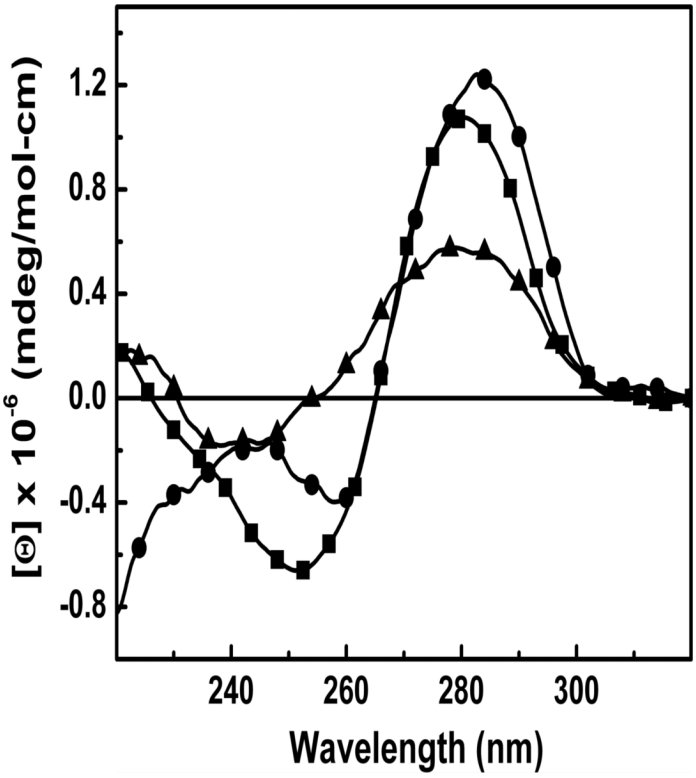

Figure 3.
Differential CD spectra in 10 mM sodium phosphate buffer for ODN-1 (■), ODN-2 (●) and ODN-3 (▲).

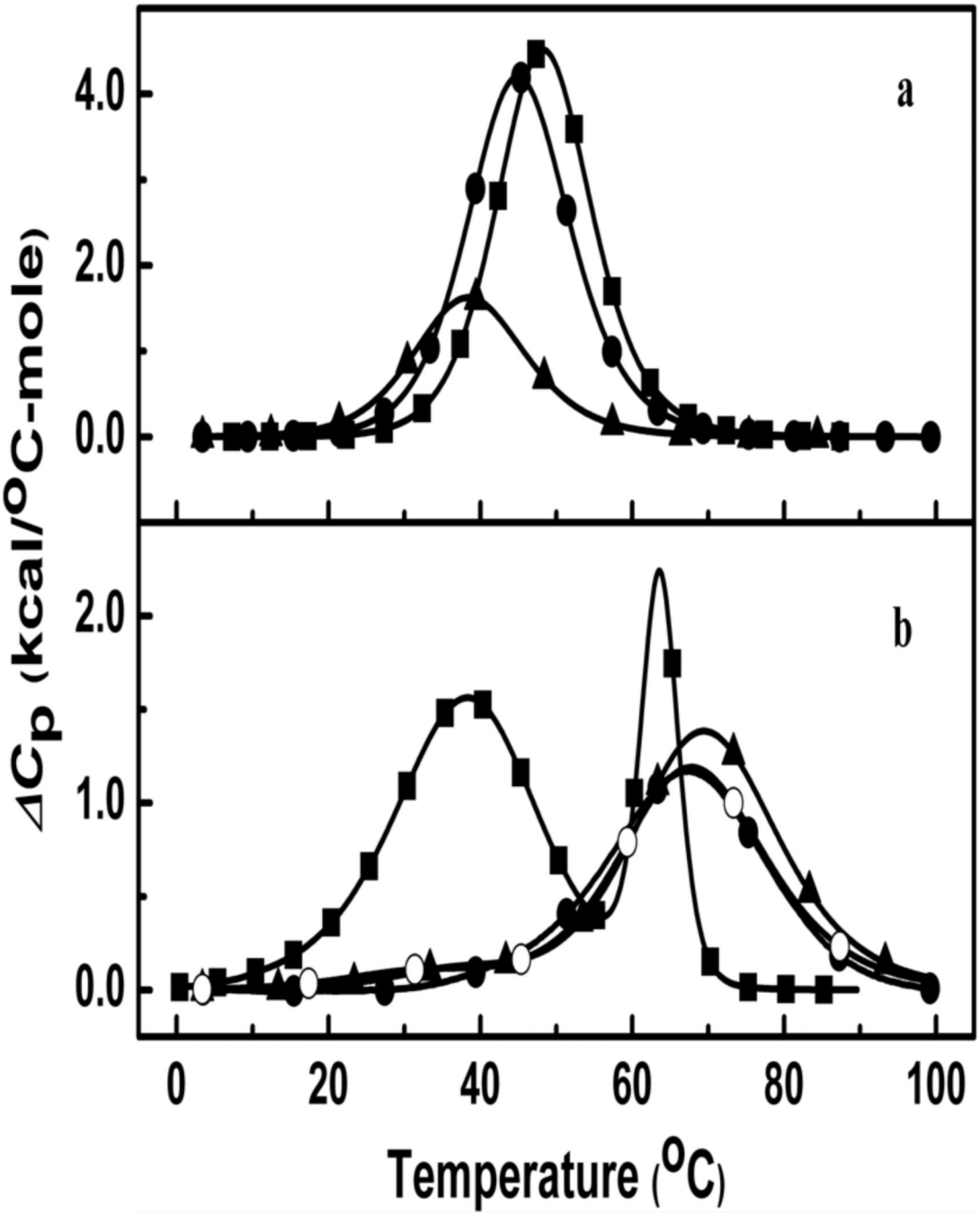

Figure 4.

(a) DSC curves in 10 mM sodium phosphate buffer (pH 7.0) at ~120 μM strand concentration for ODN-1 (■), ODN-2 (●) and ODN-3 (▲). **(b)** DSC curves in 10 mM sodium phosphate buffer (pH 7.0) at ~200 μM strand concentration for ODN-4 (■), ODN-5 (●), ODN-6 (▲) and ODN-7 (○) .

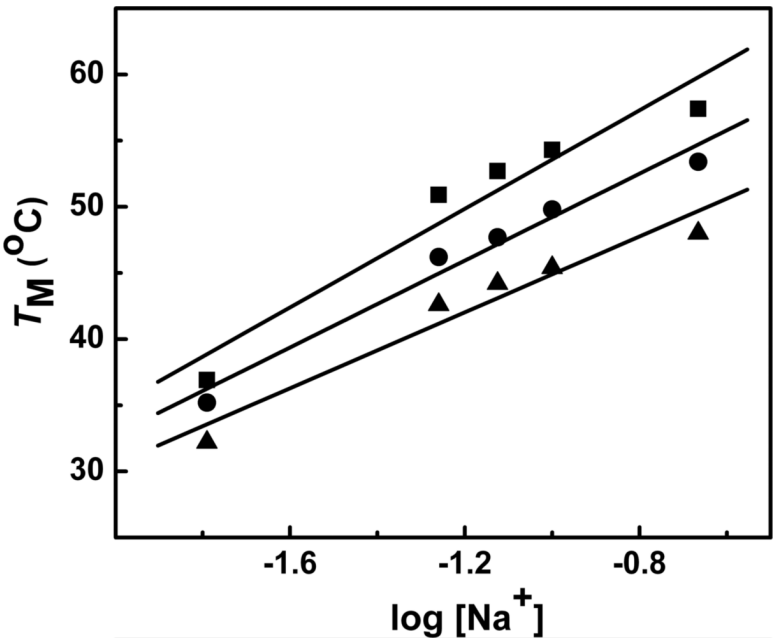

Figure 5.

T_M dependence on salt concentration for duplexes in 10 mM sodium phosphate buffer (pH 7.0), ~ 8.0 μM strand concentration for ODN-1 (■), ODN-2 (●) and ODN-3 (▲).

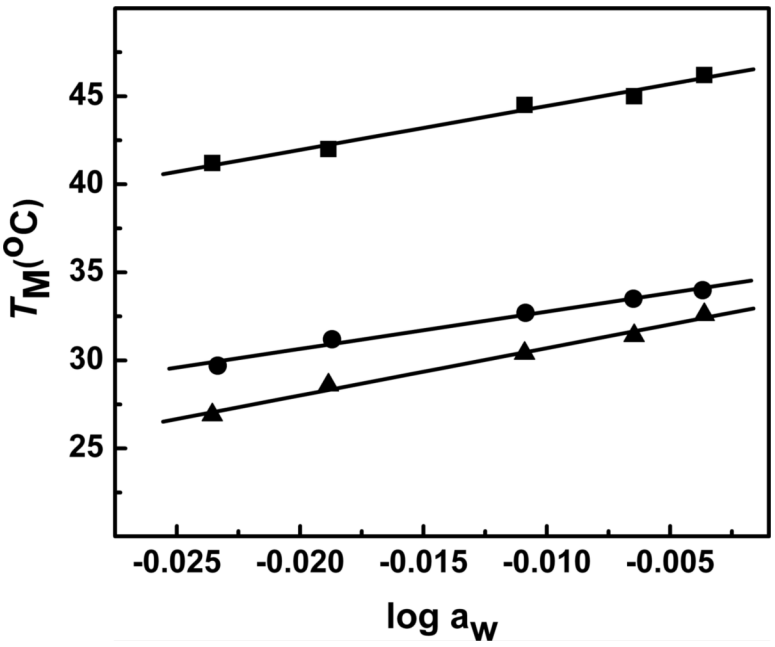

Figure 6.

T_M dependence on osmolyte concentration (as a function of ethylene glycol) in 10 mM sodium phosphate buffer (pH 7.0), ~ 8.0 μM strand concentration for ODN-1 (■), ODN-2 (●) and ODN-3 (▲).

Table 1

Structures and oligomer sequences

ODN	sequence
1	5′-GAGAGCGCTCTC-3′
2	5′-GAGZGCGCTCTC-3′
3	5′-GAGXGCGCTCTC-3′
4	5′-CGCGAATTCGCG-3′
5	5′-CGCGTTTTCGCG-3′
6	5′-CGCGAZTTCGCG-3′
7	5′-CGCGAXTTCGGC-3′

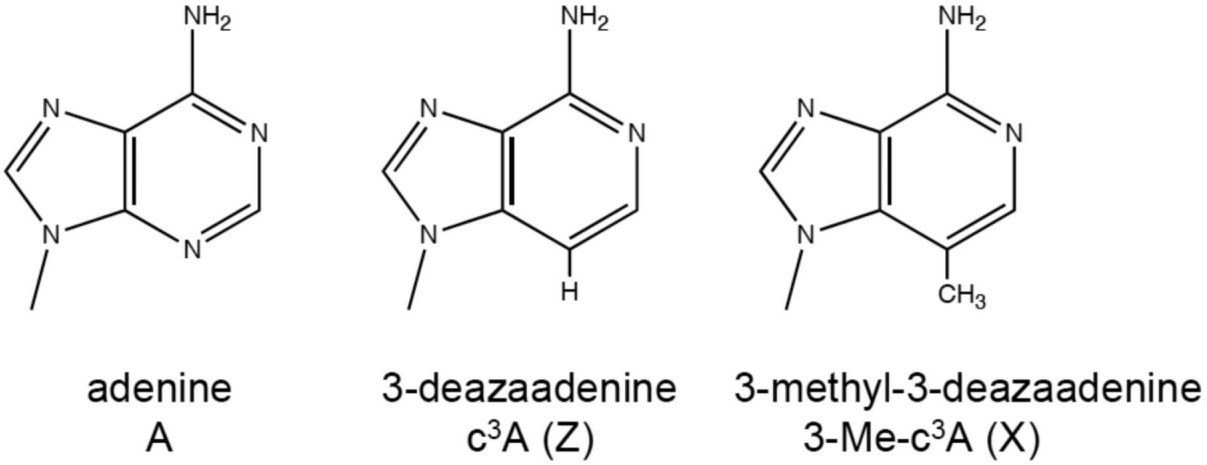

Table 2

Thermodynamic profiles for the formation of duplexes at 20 °C[a]

Oligomer	NaCl mM	T_M[b] °C	$\Delta G°$[c] kcal/mol	ΔH kcal/mol	$T\Delta S$ kcal/mol	Δn_{Na+} per mol DNA	Δn_w per mol DNA
ODN-1	10	48.7	-6.9	-78.2	-71.3	-3.4 ± 0.2	-41 ± 3
	100	66.1	-12.5	-92.0	-79.5	-3.6 ± 0.2	-43 ± 4
ODN-2	10	45.2	-6.0	-75.8	-69.8	-3.00 ± 0.1	-35 ± 3
	100	61.3	-11.3	-91.4	-80.1	-3.2 ± 0.2	-38 ± 3
ODN-3	10	38.8	-2.4	-39.0	-36.6	-1.4 ± 0.1	-24 ± 2
	100	58.8	-4.6	-39.6	-35.0	-1.2 ± 0.1	-21 ± 2
ODN-4	10	63.6	-6.9	-116.0	-109.0	-	-
ODN-5	10	68.4	-4.4	-31.0	-26.6	-	-
ODN-6	10	70.0	-5.3	-36.7	-31.4	-	-
ODN-7	10	68.9	-4.7	-32.9	-28.2	-	-

[a] Parameters are measured from UV (T_M) and DSC melting curves in 10 mM sodium phosphate buffer (pH 7.0). The observed standard deviations are: T_M (± 0.5 °C), ΔH_{cal} (± 3%), $\Delta G°_{20}$ (± 5%), $T\Delta S_{cal}$ (± 3%).

[b] 120-200 μM strand concentration.

[c] measured at 20 °C.